

# Time-Domain Macromodeling of Electromagnetic Devices Using Padé Approximation via the Lanczos Processes

Yuki Sato<sup>†</sup> and Hajime Igarashi<sup>†</sup>

<sup>†</sup>Graduate School of Information Science and Technology, Sapporo, Hokkaido University  
Kita-ku Kita 14 Nishi 9, Sapporo, 060-0814, Japan  
Email: yukisato@em.ist.hokudai.ac.jp, [igarashi@ssi.ist.hokudai.ac.jp](mailto:igarashi@ssi.ist.hokudai.ac.jp)

**Abstract**– This paper presents a time-domain macromodeling using model order reduction based on Padé approximation via the Lanczos method. In this method, the transfer function which describes input-output relation of an electromagnetic device obtained by PVL-based MOR in Laplace domain is transferred to time domain. It is shown that the transient currents of a DC-DC converter and transformer computed by this method are in good agreement with those obtained by time-domain FE analysis. Fast analysis can be performed using the present macromodel.

## 1. Introduction

Finite element method (FEM) has been widely used to analyze electromagnetic devices such as inductors, reactors and transformers. For analysis of these devices, equivalent circuits [1] and behavior models [2] are also adopted because of their light computational burden. However, it is difficult to accurately express frequency characteristics over wide frequency range using these methods. FE analysis of these devices is expected to be more accurate, while it is time-consuming.

Model order reduction (MOR) [3]-[6] has been proposed to reduce the computational time for the analysis of electromagnetic devices without deterioration of accuracy. In this method, the original system is reduced by projecting the original unknown vector onto the reduced space spanned by the basis vectors generated by MOR. It has been successfully applied to quasi-static and high frequency problems [3-5] as well as optimization problems [6]. The authors have proposed macromodel generation from FE models using MOR [7][8]. However, it has remained unclear if this method is valid for analysis of multi-port devices.

In this paper, we propose a novel method to generate macromodel of multi-port devices using MOR based on Padé approximation via the Lanczos processes (PVL) [5]. This method allows us to realize accurate and fast analysis of multi-port devices.

To test the performance, the present method is applied to modeling of an inductor in a DC-DC converter and transformer in a flyback converter which has two inputs and outputs.

## 2. Time-domain Macromodeling

Let us consider a linear system with  $p$  inputs and outputs in Laplace domain ( $s$ -domain)

$$\mathbf{N}\dot{\mathbf{x}} + \mathbf{K}\mathbf{x} = \mathbf{B}\mathbf{v} \quad (1a)$$

$$\mathbf{i} = \mathbf{L}'\mathbf{x} \quad (1b)$$

where  $\mathbf{v}$ ,  $\mathbf{i} \in \mathbf{R}^p$  are the voltage and current vectors. The unknown vector is defined by  $\mathbf{x} = [\mathbf{a}, \boldsymbol{\varphi}, \mathbf{i}]^t$ , where  $\mathbf{a}$  and  $\boldsymbol{\varphi}$  are vectors composed of magnetomotive force along element edges and scalar potential at nodes. The matrices in (1) are defined by

$$\mathbf{N} = \begin{bmatrix} \mathbf{M} & \mathbf{C} & \mathbf{0} \\ \mathbf{C}^t & \mathbf{S} & \mathbf{0} \\ \mathbf{H} & \mathbf{0} & \mathbf{0} \end{bmatrix} \in \mathbf{R}^{(n+q) \times (n+q)} \quad (2a)$$

$$\mathbf{K} = \begin{bmatrix} \mathbf{F} & \mathbf{0} & -\mathbf{H} \\ \mathbf{0} & \mathbf{0} & \mathbf{0} \\ \mathbf{0} & \mathbf{0} & \mathbf{R} \end{bmatrix} \in \mathbf{R}^{(n+q) \times (n+q)} \quad (2b)$$

where

$$M_{ij} = \int_V \kappa \mathbf{N}_i \cdot \mathbf{N}_j dV \quad (3a)$$

$$C_{ij} = \int_V \kappa \mathbf{N}_i \cdot \text{grad} \mathbf{N}_j dV \quad (3b)$$

$$S_{ij} = \int_V \kappa \text{grad} \mathbf{N}_i \cdot \text{grad} \mathbf{N}_j dV \quad (3c)$$

$$H_{ij} = \int_V \mathbf{N}_i \cdot \mathbf{J}_j dV \quad (3d)$$

$$F_{ij} = \int_V \text{rot} \mathbf{N}_i \cdot \text{rot} \mathbf{N}_j dV \quad (3e)$$

$$\mathbf{R} = \text{diag}[\mathbf{R}_1 \quad \cdots \quad \mathbf{R}_q]. \quad (3f)$$

and  $\kappa$ ,  $\mathbf{N}_i$ ,  $\mathbf{N}_j$ ,  $\mathbf{J}_j$  and  $\mathbf{R}_j$  ( $j = 1, \dots, q$ ) are the conductivity, vector and scalar interpolation functions, unit current density and dc resistance.

From (1), the admittance matrix

$$\mathbf{Y}(s) = \mathbf{L}'(\mathbf{K} + s\mathbf{N})^{-1}\mathbf{B} \quad (4)$$

is obtained. Expanding (4) around  $s_0$ , we obtain

$$Y(s_0 + \sigma) = L^t (I - \sigma A)^{-1} G \quad (5)$$

where  $s=s_0+\sigma$ ,  $A=-(K+s_0N)^{-1}N$  and  $G=(K+s_0N)^{-1}B$ . Applying spectral decomposition to A in (5), we obtain

$$Y(s_0 + \sigma) = L^t (I - \sigma S \Lambda S^{-1})^{-1} G \\ = \sum_{j=1}^{n+p} L^t S^t \frac{1}{1 - \sigma \lambda_j} S^{-1} G \quad (6)$$

where  $\lambda_j$  are the eigenvalues of A and S denotes a matrix whose columns are its eigenvectors. The transfer function for  $p$ -inputs and outputs is given by (6). It is computationally prohibitive, however, to perform spectral decomposition of A.

To modify (6), we apply Neumann series expansion to each element of  $Y(s_0+\sigma)$  to obtain

$$Y_{ij}(s_0 + \sigma) = L_i^t (I + \sigma A + \sigma^2 A^2 + \dots) g_j = \sum_{k=0}^{\infty} m_k \sigma^k \quad (7)$$

where  $L=[L_1, L_2, \dots, L_p]^t$ ,  $G=[g_1, g_2, \dots, g_p]^t$ . We still need heavy computational burden to calculate power of A in (7). To effectively calculate the power of A, we employ Lanczos method whose details and algorithm can be found in [9].

Applying Lanczos method to  $m_i$  in (7), we obtain the reduced transfer function which is equivalent to (6) as

$$Y_{ij}(s_0 + \sigma) = \sum_{k=0}^{\infty} L_i^t g_j (e_1^t T_{ij}^k e_1) \sigma^k \\ = L_i^t g_j e_1^t (I - \sigma T_{ij})^{-1} e_1 \quad (8)$$

where  $T_{ij} \in \mathbb{R}^{q \times q}$  is a tridiagonal matrix obtained by Lanczos method, and  $q$  is number of iteration for Lanczos method, and  $e_1=[1,0,\dots,0]^t$ . We now apply the spectral decomposition to  $T_{ij}$

$$Y_{ij}(s_0 + \sigma) = L_i^t g_j e_1^t (I - \sigma S_{ij} \Lambda_{ij} S_{ij}^{-1})^{-1} e_1 \\ = \sum_{m=1}^q \frac{L_i^t g_j \mu_{ijm} \nu_{ijm}}{1 - \sigma \lambda_{ijm}} \quad (9)$$

where  $\mu_{ij} = S_{ij}^t e_1$ ,  $\nu_{ij} = S_{ij}^{-1} e_1$ . Note that spectral decomposition of  $T_{ij}$  is not time-consuming because the size of  $T_{ij}$  is much smaller than that of A. The reduced transfer function can be expressed by

$$Y_{ij}(s_0 + \sigma) = \sum_{m=1}^q \frac{k_{ijm}}{\sigma - p_{ijm}} \quad (10a)$$

where

$$k_{ijm} = \frac{-L_i^t g_j \mu_{ijm} \nu_{ijm}}{\lambda_{ijm}}, \quad p_{ijm} = \frac{1}{\lambda_{ijm}} \quad (10b)$$

Because  $\sigma=s-s_0$ , the transfer function in frequency domain is given by

$$Y_{ij}(s) = \sum_{m=1}^q \frac{k_{ijm}}{s - (s_0 + p_{ijm})} \quad (11)$$

The relation between the inputs and outputs can be written by

$$\begin{bmatrix} i_1(s) \\ \vdots \\ i_q(s) \end{bmatrix} = \begin{bmatrix} Y_{11}(s) & \cdots & Y_{1q}(s) \\ \vdots & \ddots & \vdots \\ Y_{q1}(s) & \cdots & Y_{qq}(s) \end{bmatrix} \begin{bmatrix} v_1(s) \\ \vdots \\ v_q(s) \end{bmatrix} \quad (12)$$

Moreover, by applying the inverse Laplace transform to (12), we obtain the relation in time domain as

$$\begin{bmatrix} i_1(t) \\ \vdots \\ i_q(t) \end{bmatrix} = \int_0^t \begin{bmatrix} y_{11}(t-\tau) & \cdots & y_{1q}(t-\tau) \\ \vdots & \ddots & \vdots \\ y_{q1}(t-\tau) & \cdots & y_{qq}(t-\tau) \end{bmatrix} \begin{bmatrix} v_1(\tau) \\ \vdots \\ v_q(\tau) \end{bmatrix} d\tau \quad (13)$$

where

$$y_{ij}(t) = \sum_{m=1}^q k_{ijm} e^{(s_0 + p_{ijm})t} \quad (14)$$

Note that if  $s_0 + p_{ijm}$  is greater than zero, this transfer function is not passive.

### 3. Numerical Analysis

#### 3.1. Single input and output model

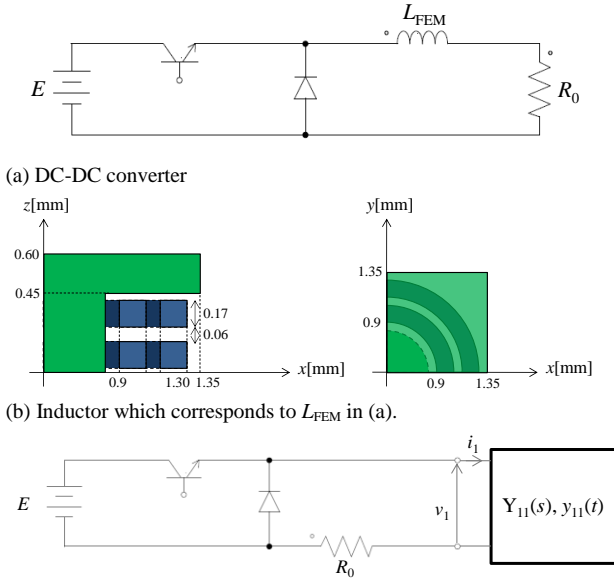
First, we consider an inductor used in the DC-DC converter which has the single input and output shown in Fig. 1 (a) and (b). The magnetic saturation in the core is taken into account by employing the frozen permeability technique whose detail is found in [10]. The driving voltage, frequency, duty factor and resistance are set to 0.35V, 100kHz, 0.9 and 0.05Ω, respectively. Eddy current flows through the coil windings of the inductor whose conductivity is set to  $5.76 \times 10^7$  S/m. Figure 1 (c) represents the macromodel constructed by the present method.

In conventional FE analysis of the DC-DC converter shown in Fig.1(a), FE equations (1) coupled with the circuit equation

$$f(v, i) = 0 \quad (15)$$

are solved in time domain. This FE analysis is time-consuming for design of inverter topology and optimization of circuit parameters. This analysis needs long computational time when the number of variable  $n$  for FE analysis is large.

By replacing the FE model with the macromodel shown in Fig. 1 (c), we can drastically reduce the computational time. After we construct the macromodel in the time domain, we simultaneously solve (13) and (15) to analyze



(c) Macromodel connected to DC-DC converter  
Fig. 1 DC-DC converter with FE model and macromodel.

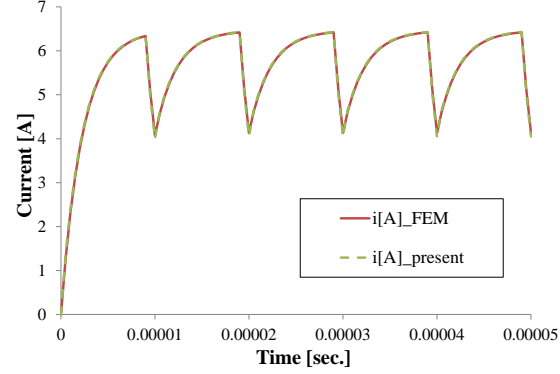


Fig. 2 Current which flows in  $R_0$ .

the DC-DC converter. In this study, we set  $q=5$ . Figure 2 shows the resistance currents where green and red lines represent the results obtained by conventional FEM and the macromodel. The both results are in good agreement during the transient analysis and steady states.

The computational time for construction of the mancomodel is about 12min. using Xeon W5590/3.2GHz(12GB RAM). Once the macromodel of  $L_{FEM}$  is constructed, we can analyze the DC-DC converter less than 1 sec. On the other hand, analysis of the DC-DC converter with FEM takes about 2 hour under the same computational environment.

### 3.2. 2-multi-port problem

We now consider a transformer model shown in Fig. 3. The relative permeability of the magnetic core is assumed to be 100 and the frequency of interest is set to  $0 < f \leq 1$ MHz.

The frequency characteristics for the impedances of transformer shown in Fig. 3 (b) are shown in Fig. 4 in which (a) and (b) represent  $Z_{11}$  and  $Z_{12}$ , respectively. The lines and dots represent results obtained by macromodel

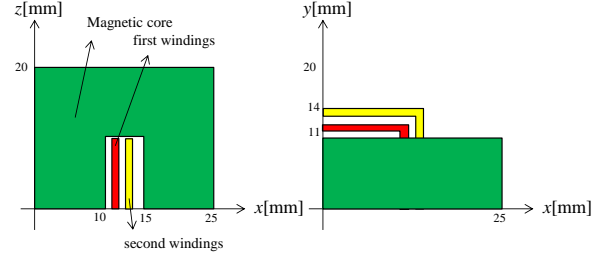
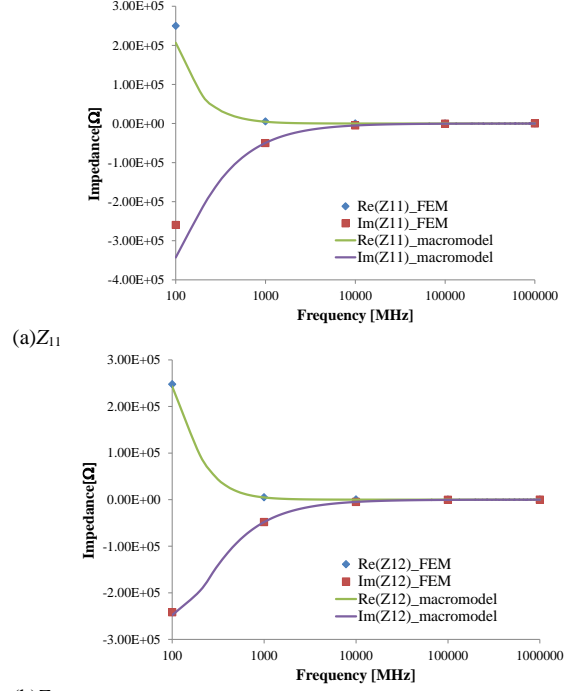


Fig. 3 transformer model.



(b) $Z_{12}$   
Fig. 4 Impedance with respect to frequency domain.

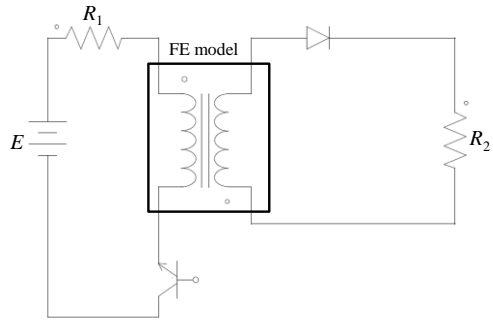


Fig. 5 Flyback converter.

( $q=15$ ) and conventional FEM. The results obtained by macromodel agree well with those obtained by FEM in the high frequency domain. In the low frequency domain, there exist differences between them. To reduce the differences,  $q$  should be increased.

Figure 5 shows a flyback converter. The diode in this converter is assumed to have  $V$ - $I$  characteristic given by

$$v_D = \begin{cases} 0.026 \times \ln\left(\frac{10^{-7} + i_D(t)}{10^{-7}}\right) & i_D(t) \geq 0 \\ 10^{12} i_D(t) & i_D(t) < 0 \end{cases} \quad (16)$$

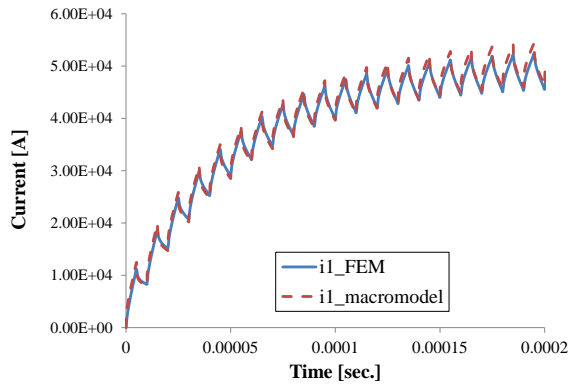
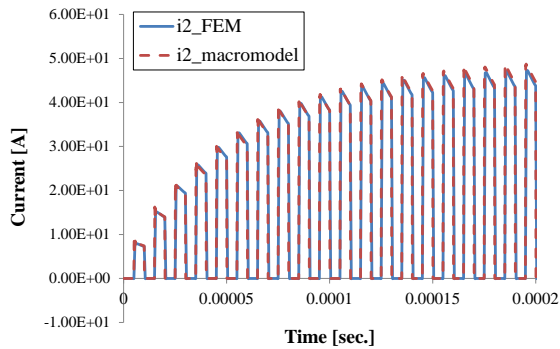
(a)  $i_1$ (b)  $i_2$ 

Fig. 6 Current with respect to time

In the analysis for the flyback converter, the driving voltage, frequency and duty factor are set to 100V, 100kHz and 0.5, respectively. The resistances  $R_1$  and  $R_2$  are set to  $10^{-3}$  and  $1\Omega$ .

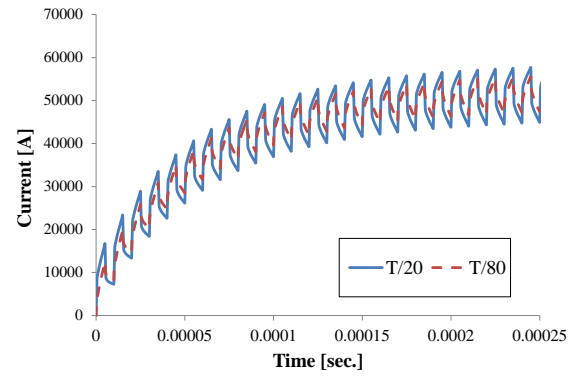
The currents  $i_1$  and  $i_2$  which flow through  $R_1$  and  $R_2$  are shown in Fig. 6 where we set  $\Delta t = T/80$  and  $\Delta t = T/20$  for present method and FEM, respectively. Both results are in good agreement during the transient and steady states. On the other hand, as can be found in Fig. 7 the discrepancies become large when we set  $\Delta t = T/20$  in the present method. It is concluded from these results that time discretization must be enough fine to reduce the errors in evaluation of the convolution integral in (13).

#### 4. Conclusion

We have proposed a construction method of the macromodel from FE model using MOR based on PVL. It has been shown that this method can be extended to analysis of multi-ports devices. It is shown that the results obtained by the macromodel are in good agreement with those obtained by full FE analysis in time and frequency domains. We can perform fast analysis using the proposed macromodels, which is effective for design and optimization of electromagnetic devices.

#### Acknowledgments

This work was supported in part by JSPS KAKENHI Grant Number 25630101 and 15J01550.

Fig. 7 Current with respect to time when  $\Delta t = T/20$  and  $T/80$ .

#### References

- [1] Y. Shindo, O. Noro, "Simple Circuit Simulation Models for Eddy Current in Magnetic Sheets and Wires," *IEEJ Trans. Fundamentals and Materials*, vol. 134, no. 4, pp. 173-181, 2014.
- [2] C. Dufour, J. Bélanger, S. Abourida, V. Lapointe, "FPGA-Based RealTime Simulation of Finite-Element Analysis Permanent Magnet Synchronous Machine Drives," *IEEE-PESC'07*, Orlando, Florida, June 2007.
- [3] Y. Sato and H. Igarashi, "Model Reduction Based on the Method of Snapshots for Eddy Current Problems," *IEEE Trans. Magn.*, vol. 49, no. 5, pp. 1697-1700, May, 2013.
- [4] T. Henneron and S. Clénet, "Model Order Reduction of Nonlinear Magnetostatic Problems Based on POD and DEI Methods," *IEEE Trans. Magn.*, vol. 50, no. 2, Feb., 2014.
- [5] P. Feldmann and R. A. Freund, "Efficient Linear Circuit Analysis by Padé Approximation via the Lanczos Process," *IEEE Trans. Computer-Aided Design*, vol. 14, no. 5, pp. 639-649, May 1995.
- [6] Y. Sato, F. Campelo and H. Igarashi, "Fast Shape Optimization of Antennas Using Model Order Reduction," *IEEE Trans. Magn.*, vol. 51, no. 3, #7204304, Mar. 2015.
- [7] Y. Sato and H. Igarashi, "Generation of Equivalent Circuit from Finite Element Model Using Model Order Reduction," *Abstract of Compumag2015* in Montreal, Canada, Jul., 2015.
- [8] T. Simotani, Y. Sato and H. Igarashi, "Generation of Equivalent Circuit from Finite Element Model of Electromagnetic Devices Using Proper Orthogonal Decomposition," *Abstract of Compumag2015* in Montreal, Canada, Jul., 2015.
- [9] C. Lanczos, "An iteration method for the solution of the eigenvalue problem of linear differential and integral operators," *J. Res. Nat. Bur. Standards*, vol. 45, pp. 255-282, 1950.
- [10] J. A. Walker, D. G. Dorrell, and C. Cossar, "Flux-linkage calculation in permanent-magnet motors using the frozen permeabilities method," *IEEE Trans. Magn.*, vol. 41, no. 10, pp. 3946-3948, Oct. 2005.